



SAHA-based novel HDAC inhibitor design by core hopping method



Lan-Lan Zang^{a,1}, Xue-Jiao Wang^a, Xiao-Bo Li^a, Shu-Qing Wang^{a,1}, Wei-Ren Xu^b,
Xian-Bin Xie^a, Xian-Chao Cheng^{a,*}, Huan Ma^a, Run-Ling Wang^{a,*}

^a Tianjin Key Laboratory on Technologies Enabling Development of Clinical Therapeutics and Diagnostics (Theranostics), School of Pharmacy, Tianjin Medical University, Tianjin 300070, China

^b Tianjin Key Laboratory of Molecular Design and Drug Discovery, Tianjin Institute of Pharmaceutical Research, Tianjin 300193, China

ARTICLE INFO

Article history:

Received 20 September 2013

Received in revised form 8 August 2014

Accepted 25 August 2014

Available online 6 September 2014

Keywords:

SAHA

Core hopping

Docking

ADMET

Molecular dynamics simulation

ABSTRACT

The catalytic activity of the histone deacetylase (HDAC) is directly relevant to the pathogenesis of cancer, and HDAC inhibitors represented a promising strategy for cancer therapy. SAHA (suberoanilide hydroxamic acid), an effective HDAC inhibitor, is an anti-cancer agent against T-cell lymphoma. However, SAHA has adverse effects such as poor pharmacokinetic properties and severe toxicities in clinical use. In order to identify better HDAC inhibitors, a compound database was established by core hopping of SAHA, which was then docked into HDAC-8 (PDB ID: 1T69) active site to select a number of candidates with higher docking score and better interaction with catalytic zinc ion. Further ADMET prediction was done to give ten compounds. Molecular dynamics simulation of the representative compound 101 was performed to study the stability of HDAC8-inhibitor system. This work provided an approach to design novel high-efficiency HDAC inhibitors with better ADMET properties.

© 2014 Elsevier Inc. All rights reserved.

1. Introduction

Cancer is a disease involving unregulated cell growth and proliferation, in which aberrant regulation of gene expression is the basis [1]. Histone deacetylases (HDACs) are a group of zinc-dependent metalloenzymes that catalyze the deacetylation of histone proteins [2]. Deacetylation results in the tighter wrapping of DNA around the histone core leading to chromatin condensation, so the accessibility of transcription factors and gene expression decreases [3]. Over-expression of HDACs induced exceedingly rich deacetylated histones, which could inhibit normal gene transcription, leading to abnormal proliferation of cancer cell [4,5]. Many studies have demonstrated that computational approaches can timely provide very useful information and insights for drug development of HDAC, such as article about the QSAR of HDAC-8 inhibitors related to SAHA [6]. The present study attempted to find novel SAHA-based HDAC inhibitors using the core hopping method and these findings might provide useful information for cancer drug development.

Vorinostat (suberoanilide hydroxamic acid, SAHA), a hydroxamate-based HDAC inhibitor, has been approved for marketing in the United States for the treatment of cutaneous T-cell lymphoma (Fig. 1) [7–10]. In the clinical use, it was found that SAHA had poor pharmacokinetic properties and adverse effects such as pulmonary embolism and anemia [11–13]. Thus there has been a growing interest in developing novel inhibitors with less toxicity and improved pharmacokinetic properties.

A general description of known HDAC inhibitors consists of: (a) a cap group that interacts with a peripheral binding site adjacent to the zinc ion; (b) a zinc-binding group (ZBG) that coordinates to the catalytic zinc ion within the active site; and (c) a linker group that binds with hydrophobic tunnel residues and positions the ZBG and a capping group for interactions in the active site (Fig. 1) [14].

According to the description of SAHA, based on the core-hopping strategy, the cap group, linker and ZBG were respectively replaced by various moieties to form novel molecules. These molecules were evaluated for their docking scores and ADMET properties to select ten candidates that were better than SAHA. One of these candidates, compound 101, was further studied by 10 ns molecular dynamics (MD) simulations to evaluate the binding stability with HDAC enzyme.

* Corresponding authors. Tel.: +86 022 83336658.

E-mail addresses: chengxianchao@aliyun.com (X.-C. Cheng), wangrunling@tjmu.edu.cn (R.-L. Wang).

¹ These authors contributed equally to this work.

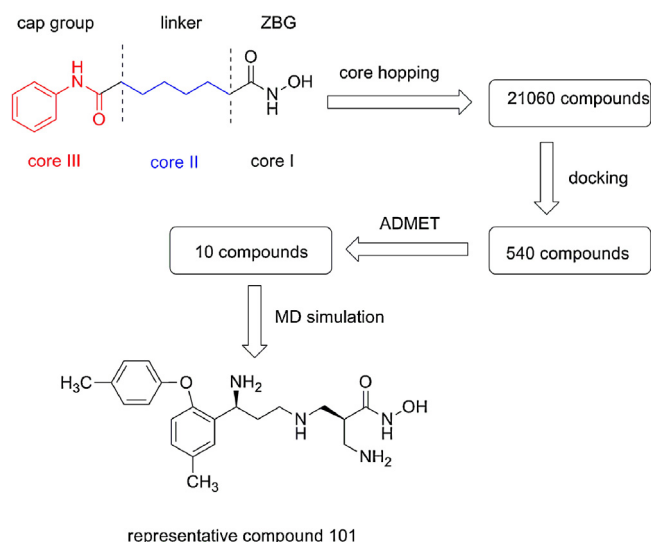


Fig. 1. The general research flowchart.

2. Materials and methods

2.1. Protein structure and database

The crystal structure of HDAC-8 binding the ligand SAHA with higher resolution (2.91 Å) and less missing residues in the sequence was downloaded from the Protein Data Bank [15,16] (PDB ID: 1T69), which was released by Somoza et al. [17]. The binding pocket of HDAC-8 was generated using co-crystallized ligand-coordinated space. The fragment database derived from ZINC [18] was used for core hopping research.

2.2. Core hopping method

The structure of SAHA was modified by core hopping method, in which the core III and core II were derived from ZINC fragment database (Fig. 2) [18], and core I was replaced by reported zinc binding groups (hydroxamate, carboxylate, hydroxyurea, etc.) (Fig. 2) [19]. By combination of the core III, core II and core I, various compounds were constructed, which were then docked into the HDAC-8 active site to evaluate their binding effects. The core hopping was performed by combiglide package in Schrodinger [20], which was a type of scaffold replacement module [21–23].

2.3. Docking method

The surflex-dock [24–26] module in the SYBYL-X 1.1 [27] package was used for the docking analysis [28]. This docking mode is flexible docking, and it is a useful medium to probe the interaction of a protein receptor with its ligand and reveal their binding mechanism as demonstrated by a series of studies [29–37]. Surflex-dock uses an empirical scoring function and a patented search engine to dock ligands into a protein's binding site. What is more, it is a weighted sum of non-linear functions involving van der Waals surface distances between the appropriate pairs of exposed protein and ligand atoms. It is particularly successful at removing false positive results and then be used to narrow down the screening pool significantly, while still holding a large number of active compounds [28,38].

Before the docking experiment, the ligands were prepared via the ligand structure preparation module [39–41], in which “sanitize” was chosen as the default preparation protocol. Its function was doing a general cleanup of the structures involving filling valences, checking for correctness, standardizing, removing

duplicates and producing only one molecule per input structure. The prepared ligands were exported as SLN format, in which the ligand SAHA as a positive control was also included. As for the receptor preparation, the hydrogen and missing atoms were added and solvent molecules were removed. The zinc ion and associated amino acid residues were treated by “Set Protonation Type”, and the necessary charges were added, which was then energy minimized to obtain the docking receptor [42].

Docking is guided by the protocol, and it is a computational representation of a proposed ligand that interacts with the binding site [43]. The protocol is not meant to be an absolute docking envelope. Its purpose is to direct the initial placement of the ligand during the docking process. Docked ligands are scored in the context of the receptor, not in the context of the protocol [44]. In this paper, the docking protocol was constructed by ligand mode [44]. In this mode, the coordinate space of the extracted co-crystallized ligand was used as the receptor binding pocket [45–47]. Two parameters determining the extent of the binding pocket, a threshold value of 0.50 and a bloat value of 1 Å, were also established.

During the docking process, surflex-dock's initial implementation used the Hammerhead procedure to screen for the binding of flexible molecules to a protein binding site. For each ligand, the Hammerhead procedure is as follows: (a) Generate the ligand fragments. This operation reduces the conformational space that must be explored; (b) Align the fragments onto the protocol probes; (c) Dock the remainder of the ligand's fragments [48]. Each ligand induced various conformational changes to fit the receptor, while the receptor conformation was stable and did not change during the docking process (Fig. 3). SYBYL software selected the top 20 conformations for each ligand and displayed them in the docking result list [42]. The binding pose with the highest total score was taken into consideration for ligand–receptor interaction, which was analyzed by the manual examination and comparison to SAHA.

2.4. ADMET prediction

To be a successful drug, compounds should not only be active against a target, but also possess appropriate ADMET (absorption, distribution, metabolism, excretion and toxicity) properties. The ADMET module of Discovery studio 3.1 was used to predict these properties. The compounds database was prepared as mol2 file, which was then imported to the ADMET descriptors, Toxicity Prediction Extensible and Toxicity Prediction TOPKAT, respectively. The job was submitted and predicted results were obtained.

2.5. Molecular dynamics simulation

By studying the internal motions of proteins and DNA [49], many marvelous biological functions and their profound dynamic mechanisms [50], such as switch between active and inactive states, cooperative effects [51], allosteric transition, intercalation of drugs into DNA, and assembly of microtubules, can be revealed, and briefed in a recent discussion [52]. Likewise, we should combine the static structures concerned and the dynamical information obtained by simulating their internal motions or dynamic process to really understand the action mechanism of receptor–ligand binding mode. To realize this, the MD simulation [19] is one of the feasible tools.

In order to examine the binding stability of representative compound 101 with HDAC-8 active site, the molecular dynamic simulations were performed by using GROMACS 4.0 package for Linux. GROMACS 96–53a6 force fields [53] and the periodic boundary conditions (PBC) were employed in the MD simulations.

The topology files and charges for the ligand atoms were generated by the Dundee PRODRG 2.5 Server (beta) [54]. Before starting the simulations, all the models were solvated with the explicit

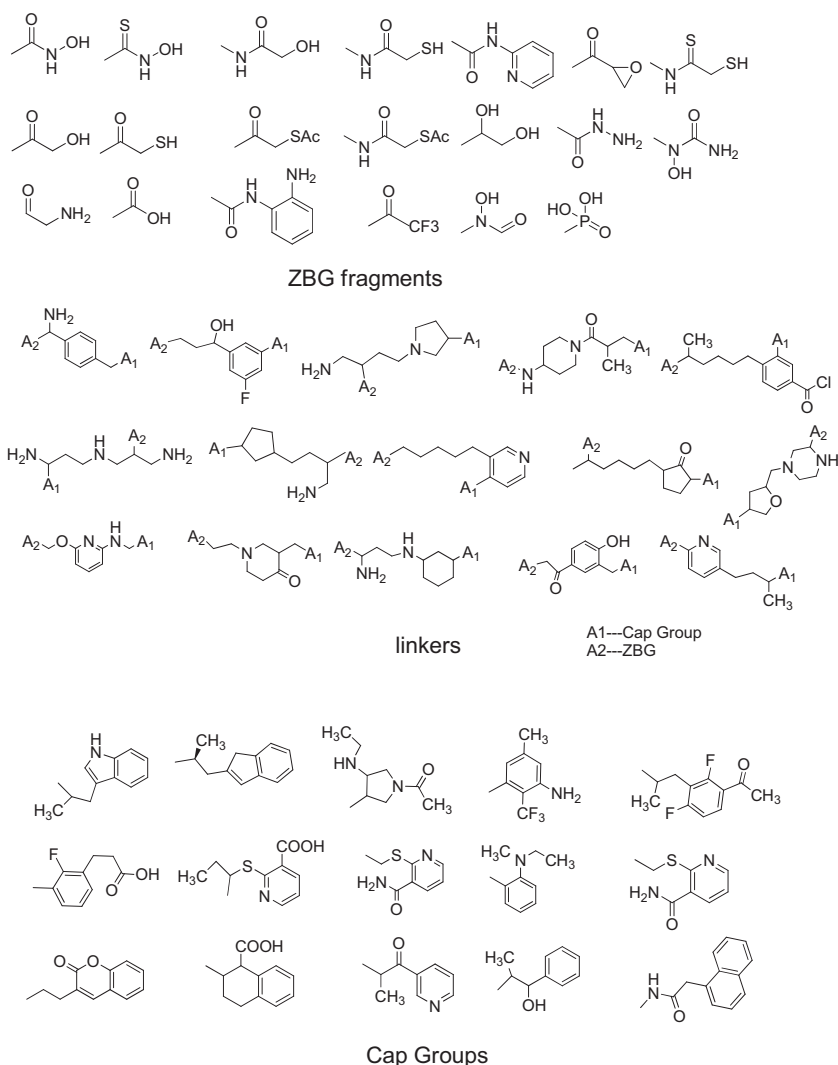


Fig. 2. Parts of core hopping fragments.

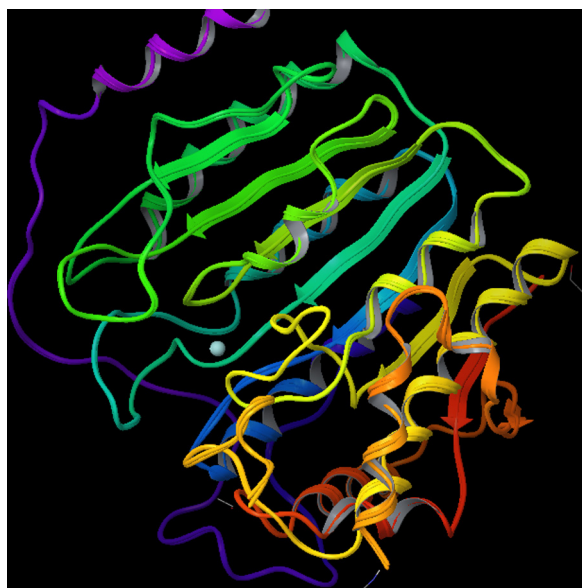


Fig. 3. Superposition of native HDAC-8 (narrow strings in α helix and β sheet) and docked HDAC-8 (wide strings in α helix and β sheet).

simple point charge (SPC) water in a cubic box [55,56]. The system was neutralized with five sodium ions replacing the five SPC water molecules. Subsequently, the energy minimization was performed for the system by using the steepest descents approach until reaching a tolerance of 100 kCal/mol. Then the systems were heated to 300 K within 10 ps, and we chose a longer heating time of 100 ps to detect the systems steady or not, followed by another 100 ps with NPT equilibration treatment to make the balance between the temperature and pressure. Then, the 10 ns MD simulations were carried out with a time step of 1 fs, and the corresponding coordinates were stored every 100 fs. The particle mesh Ewald (PME) algorithm was used to calculate the electrostatic interactions. All simulations were run under constant temperature (300 K), periodic boundary conditions and NVT ensembles. All hydrogen-heavy atom bonds were constrained by using the Linear Constraint Solver (LINCS) algorithm.

3. Results and discussion

3.1. Ligand binding domain of HDAC-8

The protein database bank (PDB) demonstrated the ligand binding domain of the HDAC-8 (PDB ID:1T69), which was surrounded by 11 α helix (the red helix in Fig. 4A) and 8 paralleled β sheet (the

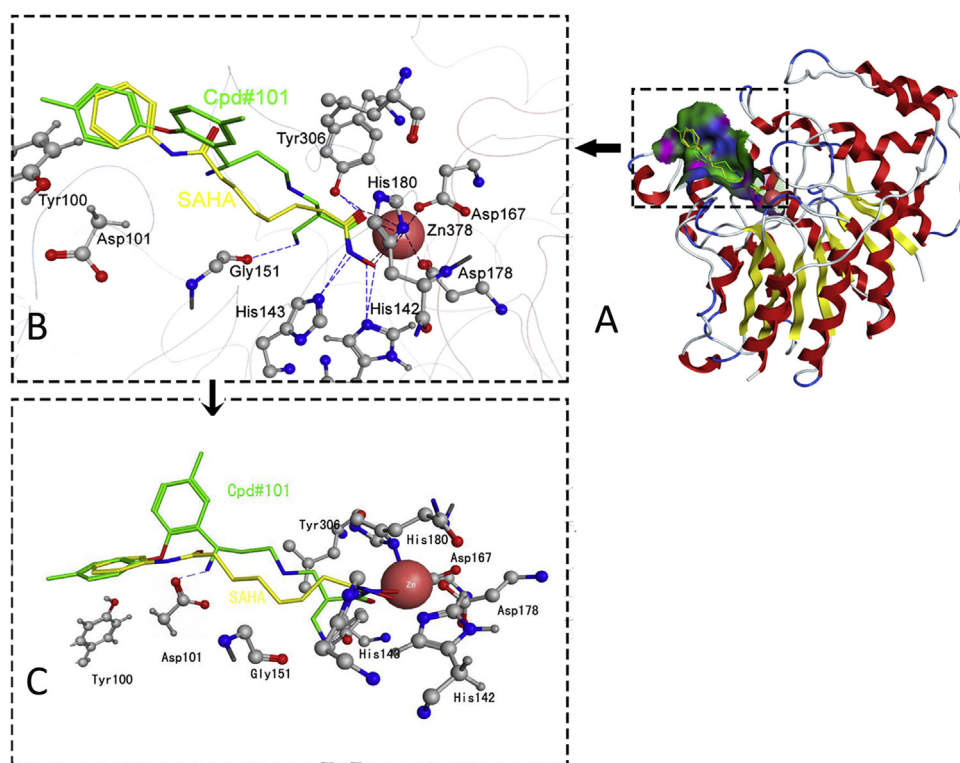


Fig. 4. (A) The conformation and interaction map of HDAC-8 with SAHA (small molecule colored in yellow among the pocket) and compound 101 (small molecule colored in green among the pocket); (B) A close-up view of binding site (H-bonds between ligands and protein were highlighted in blue, while the contact between Zn378 and ligands were colored in purple); (C) The rotation of B (H-bond between ligands and protein was highlighted in blue).

yellow strip in Fig. 4A). The ligand binding domain of HDAC-8 was about 12 Å long narrow hydrophobic channel, which was constituted by residues of Phe152, Phe208, His180, Gly151, Met274 and Tyr306, and the catalytic zinc ion (ZN378) was at the bottom of the hydrophobic channel.

3.2. Core hopping and docking

After optimization by core-hopping in Schrodinger 2009, about 21,060 compounds were identified, which were then docked to the HDAC-8 active site using the surflex-dock of Sybyl-X 1.1. At the same time, we docked SAHA and its analogs that entered clinical trial, including PDX101 (Phase II) [57], LBH589 (Phase III) [58] and LAQ824 (Phase I) [59] (Table 1). A total of 540 candidates with higher docking scores and more steady interaction with Zn378 than SAHA were identified, among which top ten candidates with better ADMET properties were listed in Table 2. Surflex-dock scores (total scores) are expressed in $-\log 10$ (Kd) units to represent the binding affinities. The results showed that the calculated values of SAHA analogs (Table 1) were in agreement with the IC_{50} values, supporting the idea that the surflex-dock values were consistent with the activities of the compounds [60,61]. Based on this idea, we analyzed the compounds that had better binding affinities, the docking model of representative compound 101 and SAHA with the active site of HDAC-8 was also shown in Fig. 4.

Table 1
The docking scores and IC_{50} values of SAHA and candidate drugs.

Entry	Docking score—lg (Kd)	IC_{50} (nM)
Vorinostat (SAHA)	9.87	1524
Panobinostat (LBH589)	10.04	248
Belinostat (PDX101)	10.11	216
LAQ824	10.32	162

The docking result in this study revealed that the better interaction of these ligands than SAHA might be due to coulomb attraction of the hydroxamate ZBG toward catalytic zinc ion. The zinc ion was coordinated at five points with the side chain O of Asp267 and Asp178, the N of His180, the carbonyl and the hydroxyl oxygen of the ligand's hydroxamate group, respectively, forming a pentacoordinate geometry (Fig. 4B). As seen in Table 1, the hydroxyl oxygen of the hydroxamate group in the compound 101 is at 1.94 Å distance from Zn378, and the carbonyl oxygen of the hydroxamate group is at 1.98 Å distance from Zn378, both of which were closer than that of SAHA, thus forming a better interaction with the enzyme active site [62].

The hydroxamate group of compound 101 also formed hydrogen bond interactions with Tyr306 (1.87 Å), His142 (2.13 Å) and His143 (2.73 Å and 2.02 Å), respectively, which was similar to the binding mode of SAHA.

As for the linker and cap group of compound 101, hydrophobic interactions played a major role in the stability of the ligand–protein complex, directing the hydroxamate group to the tunnel bottom to coordinate with zinc ion. In addition, the hydroxy at the cap group of compound 101 formed hydrogen bonds with Asp101 (2.02 Å) (Fig. 4C) and Gly151 (1.77 Å) (Fig. 4B), respectively, making the binding more steadily.

3.3. ADMET prediction

The ADMET properties of compounds could be predicted by the molecular weight (MW), number of hydrogen bond donors ($nOHNH$), number of hydrogen bond acceptors (nON), the octanol–water partition coefficient ($AlogP_{98}$), the polar surface area (PSA-2D), and aqueous solubility (QplogS). According to the Lipinski's rule of five [63], the molecular weight should be less than 500, the number of hydrogen bond donors ($nOHNH$) should be no more than 5, the number of hydrogen bond acceptors (nON) should be no

Table 2
The docking results of top ten candidates modified from SAHA.

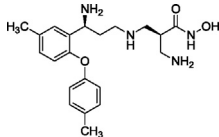
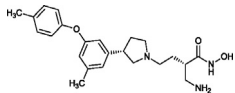
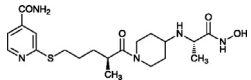
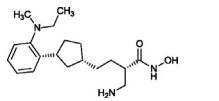
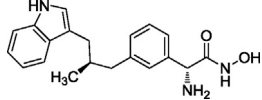
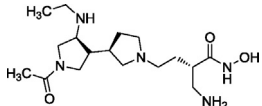
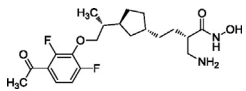
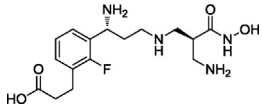
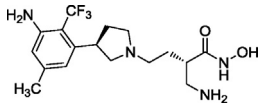
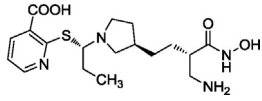
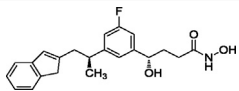
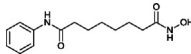
Entry	Structure	Docking score—lg (Kd)	Zinc binding distance (Å) ^a	Hydrogen bond distance (Å) ^b
Cpd#101		12.25	d—OH: 1.94 dC=O: 1.98	His142:2.13; His143(—OH):2.73; His143(—NH):2.02;Tyr306:1.87; Gly151:1.77; Asp101:2.02
Cpd#869		11.20	d—OH: 2.00 dC=O: 2.00	His142:2.13; His143(—OH):2.73; His143(—NH):1.98; Tyr306:1.86; Tyr100:1.95
Cpd#69		10.96	d—OH: 1.85 dC=O: 2.19	His142:2.05; His142(—OH):2.88; His143(—NH):1.83; Tyr306:2.12; Tyr100:2.07; Phe208:2.01
Cpd#545		10.70	d—OH: 1.95 dC=O: 2.08	His142:2.04; His143(—OH):2.64; His143(—NH):1.98; Tyr306:2.13; Gly151:2.29
Cpd#90		10.65	d—OH: 1.91 dC=O: 2.00	His142:2.19; His143(NH):1.82; Tyr306:1.84; Gly151:1.85
Cpd#1292		10.29	d—OH: 2.00 dC=O: 2.03	His142:2.19; His143(—OH):2.65; His143(—NH):2.00; Tyr306(C=O):1.99; Tyr306(NH2):1.99; Gly151:2.05
Cpd#1025		10.22	d—OH: 2.05 dC=O: 1.96	His142:1.96; His143(—OH):2.82; His143(—NH):1.90; Tyr306:1.95; Gly151:1.99
Cpd#1149		10.21	d—OH: 1.97 dC=O: 2.05	His142:2.30; His143(—OH):2.62; His143(—NH):2.05; Tyr306:1.89; Asp101:2.03; Tyr100:1.85
Cpd#372		10.03	d—OH: 1.93 dC=O: 1.97	His142:2.10; His143(—OH):2.83; His143(—NH):1.98;Tyr306(C=O):1.88; Tyr306(NH2):2.05;Tyr100:2.06; Gly151:2.45
Cpd#232		10.13	d—OH: 1.92 dC=O: 1.97	His142:2.18; His143(—OH):2.71; His143(—NH):2.03;Tyr306:1.88; Gly151:1.709; Asp101:1.84

Table 2 (Continued)

Entry	Structure	Docking score—lg (Kd)	Zinc binding distance (Å) ^a	Hydrogen bond distance (Å) ^b
Cpd#117		9.98	d—OH: 1.91 dC=O: 2.04	His142:2.09; His143(—NH):1.86; Tyr306:1.80
SAHA		9.87	d—OH: 2.07 dC=O: 2.14	His142:2.20; His143(—OH):2.61; His143(—NH):1.95; Tyr306:2.16

^a Zinc binding distance is acceptable under 2.14 Å [65].^b Hydrogen bond distance (N—H...O, O—H...O and so on) is acceptable under 3.20 Å [66–69].

Table 3

The ADMET prediction results of top ten candidates modified from SAHA.

Entry	MW (g/mol)	AlogP ₉₈ ^a	PSA-2D ^b	QplogS ^c	nON ^d	nOHNH ^e	SL3 computed probability of mutagenicity (%)
Cpd#101	386.493	−2.585	121	−0.109	6	5	0
Cpd#869	373.399	−2.319	113	−0.182	8	4	0
Cpd#69	411.472	2.830	106	−3.356	9	3	0
Cpd#545	333.473	2.719	81	−2.269	4	3	0
Cpd#90	337.421	3.203	92	−1.833	5	4	0
Cpd#1292	372.414	−2.121	122	−0.255	8	4	0
Cpd#1025	398.449	2.717	103	−2.595	6	3	0
Cpd#1149	392.540	0.817	137	−0.423	6	5	0
Cpd#372	409.502	−0.187	139	−2.250	9	5	0
Cpd#232	387.426	0.199	116	−0.804	8	4	0
Cpd#117	369.435	3.704	72	−4.360	6	3	0
SAHA	264.324	1.838	78	−2.147	5	3	0.005

^a AlogP₉₈ means atom-based LogP (octanol/water) [70].^b PSA-2D means 2D fast polar surface area [71].^c QplogS means predicted aqueous solubility.^d nON means number of hydrogen bond acceptors.^e nOHNH means number of hydrogen bonds donors.

more than 10, and the octanol–water partition coefficient (AlogP₉₈) should be less than 5. As seen in Table 3, the candidate compounds accorded with these rules. In addition, they fell into the acceptable ranges of PSA-2D (7–200) and QplogS (−6.5 to 0.5), thus possessing good bioavailability.

Further toxicity analysis showed that the probabilities of mutagenicity of most candidate compounds were lower than SAHA (SL3 = 0.005). This parameter was also taken into consideration to identify better inhibitors.

3.4. Molecular dynamics trajectory analysis

Molecular dynamics simulations were performed by Gromacs 4.0 to evaluate the system stability of the HDAC8-compound 101 complex, HDAC8-SAHA complex and HDAC8, respectively. The temperature fluctuated from 299 K to 305 K and the systems were steady as seen in Fig. 5.

The root mean square deviation (RMSD) versus the simulation time was considered as a significant criterion to evaluate the stability of dynamic behavior. As shown in Fig. 6A, the final RMSD values for three simulation trajectories were less than 5 Å, indicating that the receptor structures had reached the equilibrium states with little alterations during the entire simulations. In addition, the RMSD for HDAC8-101 system (red) is the lowest among these three simulation trajectories after 3 ns, indicating that the flexibility of HDAC8 was decreased and the activity of HDAC-8 might be inhibited by binding compound 101.

As a significant parameter to investigate the motion of key residues interacted with the ligand, the root mean square fluctuations (RMSF) for all the side chain atoms of HDAC-8

active site were calculated. As shown in Fig. 6B, the RMSF values of key residues with compound 101 were 1.326 Å (His142), 1.469 Å (His143), 2.969 Å (Asp178), 2.714 Å (His180) and 1.996 Å (Asp267), respectively, lower than the apo form and SAHA-binding form. These values indicated that compound 101 restricted the movement of some key residues more than that of SAHA, and HDAC-8 was more stable after binding compound 101 [22].

To check whether the chelating interactions between zinc and the ligands were reasonable or not during the course of the MD simulation [64], the analysis of distances between zinc and bidentate ligands were required. As Fig. 7 showed, the Zn²⁺–O₁ and

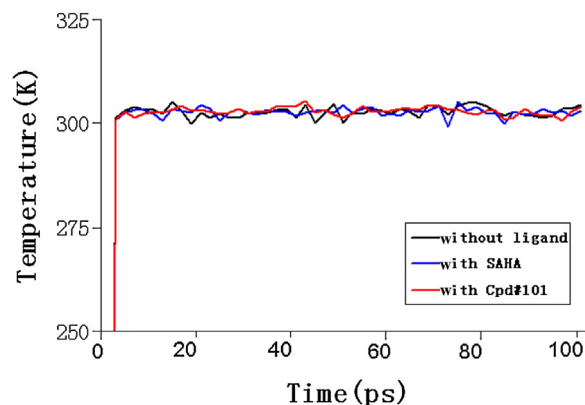


Fig. 5. The temperature balance of molecular dynamic simulations.

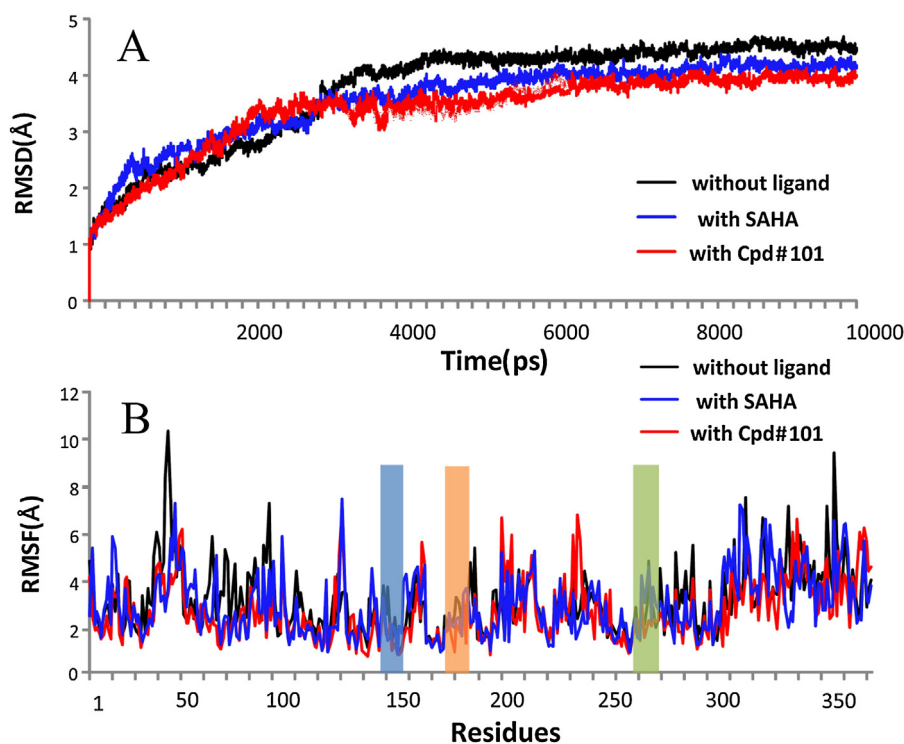


Fig. 6. The RMSD (A) and RMSF (B) results of molecular dynamic simulations.

Zn^{2+} – O_2 distances fluctuated around 2.1 and 2.2 Å during the 10 ns MD simulation with SAHA. These values nearly matched the docking results (2.07 Å and 2.14 Å), indicating that the chelating interaction existed during the molecular dynamics to make the receptor–ligand complex stable. As for the Zn^{2+} – O_1 and Zn^{2+} – O_2 distances with compound 101, it also had the same case. These results demonstrated that both ligands had good chelating interaction with the zinc ion during the 10 ns MD simulation time, and compound 101 bound steadily to the HDAC-8 active site. Compound 101 was anticipated to be a promising drug candidate for further experimental investigation.

4. Conclusion

Starting from SAHA as the guiding molecule, using core hopping strategy, docking and ADMET prediction technique, a series of novel HDAC inhibitors were designed in this study. Compared with SAHA, the top ten candidate compounds possess higher HDAC-8 docking scores, better pharmacokinetic properties and lower toxicity. Molecular dynamic simulations of the representative compound 101 showed that compound 101 bound steadily to the HDAC-8 active site and might be a more potent HDAC-8 inhibitor than SAHA. Further synthesis and assay of these compounds were underway in our lab.

Acknowledgements

This work was supported by National Natural Science Foundation of China (21202120), China Postdoctoral Science Foundation funded project (2012T50237 and 20100480655), Tianjin Medical University New Century Talent Foundation and Tianjin Medical University Undergraduate Research Project. The authors also thank the anonymous reviewers for their valuable suggestions.

References

- [1] T. Suzuki, N. Miyata, Non-hydroxamate histone deacetylase inhibitors, *Curr. Med. Chem.* 12 (2005) 2867–2880.
- [2] P. Dey, Chromatin remodeling, cancer and chemotherapy, *Curr. Med. Chem.* 13 (2006) 2909–2919.
- [3] G. Bora-Tatar, D. Dayangac-Erden, A.S. Demir, S. Dalkara, K. Yelekci, H. Erdem-Yurter, Molecular modifications on carboxylic acid derivatives as potent histone deacetylase inhibitors: activity and docking studies, *Bioorg. Med. Chem.* 17 (2009) 5219–5228.
- [4] C.B. Yoo, P.A. Jones, Epigenetic therapy of cancer: past, present and future, *Nat. Rev. Drug Discovery* 5 (2006) 37–50.
- [5] C.M. Grozinger, S.L. Schreiber, Deacetylase enzymes: biological functions and the use of small-molecule inhibitors, *Chem. Biol. Interact.* 9 (2002) 3–16.
- [6] S. Hanessian, L. Auzzas, G. Giannini, M. Marzi, W. Cabri, M. Barbarino, L. Vesce, C. Pisano, Omega-alkoxy analogues of SAHA (vorinostat) as inhibitors of HDAC:

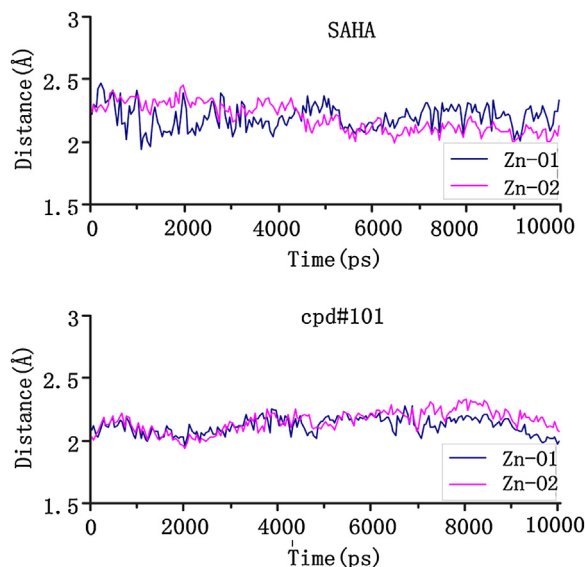


Fig. 7. Zn^{2+} –oxygen distance fluctuation in HDAC8-SAHA complex and HDAC8-compound 101 complex.

- a study of chain-length and stereochemical dependence, *Bioorg. Med. Chem. Lett.* 17 (2007) 6261–6265.
- [7] T. Jenuwein, C.D. Allis, Translating the histone code, *Science* 293 (2001) 1074–1080.
 - [8] M.S. Finnin, J.R. Donigan, A. Cohen, V.M. Richon, R.A. Rifkind, P.A. Marks, R. Breslow, N.P. Pavletich, Structures of a histone deacetylase homologue bound to the TSA and SAHA inhibitors, *Nature* 401 (1999) 188–193.
 - [9] P.A. Marks, R. Breslow, Dimethyl sulfoxide to vorinostat: development of this histone deacetylase inhibitor as an anticancer drug, *Nat. Biotechnol.* 25 (2007) 84–90.
 - [10] W.K. Kelly, O.A. O'Connor, P.A. Marks, Histone deacetylase inhibitors: from target to clinical trials, *Expert Opin. Invest. Drugs* 11 (2002) 1695–1713.
 - [11] K. Traynor, Vorinostat A novel therapy for the treatment of cutaneous T-cell lymphoma, *Am. J. Health Syst. Pharm.* 67 (2010) 1136.
 - [12] A.M. Traynor, S. Dube, J.C. Eickhoff, J.M. Kolesar, K. Schell, M.S. Huie, D.L. Groteluschen, S.M. Marcotte, C.M. Hallahan, H.R. Weeks, G. Wilding, I. Espinoza-Delgado, J.H. Schiller, Vorinostat (NSC# 701852) in patients with relapsed non-small cell lung cancer: a Wisconsin Oncology Network phase II study, *J. Thorac. Oncol.* 4 (2009) 522–526.
 - [13] B.J. Schneider, G.P. Kalemkerian, D. Bradley, D.C. Smith, M.J. Egorin, S. Daignault, R. Dunn, M. Hussain, Phase I study of vorinostat (suberoylanilide hydroxamic acid, NSC 701852) in combination with docetaxel in patients with advanced and relapsed solid malignancies, *Invest. New Drugs* 30 (2012) 249–257.
 - [14] Y. Itoh, A. Shimazu, Y. Sadzuka, T. Sonobe, S. Itai, Novel method for stratum corneum pore size determination using positron annihilation lifetime spectroscopy, *Int. J. Pharm.* 358 (2008) 91–95.
 - [15] H.M. Berman, T. Battistuz, T.N. Bhat, W.F. Bluhm, P.E. Bourne, K. Burkhardt, Z. Feng, G.L. Gilliland, L. Iype, S. Jain, P. Fagan, J. Marvin, D. Padilla, V. Ravichandran, B. Schneider, N. Thanki, H. Weissig, J.D. Westbrook, C. Zardecki, The Protein Data Bank, *Acta Crystallogr. D: Biol. Crystallogr.* 58 (2002) 899–907.
 - [16] J. Westbrook, Z. Feng, S. Jain, T.N. Bhat, N. Thanki, V. Ravichandran, G.L. Gilliland, W. Bluhm, H. Weissig, D.S. Greer, P.E. Bourne, H.M. Berman, The Protein Data Bank: unifying the archive, *Nucleic Acids Res.* 30 (2002) 245–248.
 - [17] J.R. Somoza, R.J. Skene, B.A. Katz, C. Mol, J.D. Ho, A.J. Jennings, C. Luong, A. Arvai, J.J. Buggy, E. Chi, J. Tang, B.C. Sang, E. Verner, R. Wynands, E.M. Leahy, D.R. Dougan, G. Snell, M. Navre, M.W. Knuth, R.V. Swanson, D.E. McRee, L.W. Tari, Structural snapshots of human HDAC8 provide insights into the class I histone deacetylases, *Structure* 12 (2004) 1325–1334.
 - [18] J.J. Irwin, B.K. Shoichet, ZINC—a free database of commercially available compounds for virtual screening, *J. Chem. Inf. Model.* 45 (2005) 177–182.
 - [19] K. Chen, L. Xu, O. Wiest, Computational exploration of zinc binding groups for HDAC inhibition, *J. Org. Chem.* 78 (2013) 5051–5055.
 - [20] Schrodinger-LLC, Schrodinger Suite 2009, Virtual Screening Workflow; Glide version 5.5, Schrodinger, LLC, New York, NY, 2009.
 - [21] X.B. Li, S.Q. Wang, W.R. Xu, R.L. Wang, K.C. Chou, Novel inhibitor design for hemagglutinin against H1N1 influenza virus by core hopping method, *PLoS One* 6 (2011) e28111.
 - [22] Y. Ma, S.Q. Wang, W.R. Xu, R.L. Wang, K.C. Chou, Design novel dual agonists for treating type-2 diabetes by targeting peroxisome proliferator-activated receptors with core hopping approach, *PLoS One* 7 (2012) e38546.
 - [23] L.S. Zhang, S.Q. Wang, W.R. Xu, R.L. Wang, J.F. Wang, Scaffold-based pan-agonist design for the PPARalpha, PPARbeta and PPARgamma receptors, *PLoS One* 7 (2012) e48453.
 - [24] R. Spitzer, A.N. Jain, Surflex-Dock: docking benchmarks and real-world application, *J. Comput.-Aided Mol. Des.* 26 (2012) 687–699.
 - [25] A.N. Jain, Surflex-Dock 2.1: robust performance from ligand energetic modeling, ring flexibility, and knowledge-based search, *J. Comput.-Aided Mol. Des.* 21 (2007) 281–306.
 - [26] M.A. Miteva, W.H. Lee, M.O. Montes, B.O. Villoutreix, Fast structure-based virtual ligand screening combining FRED, DOCK, and surflex, *J. Med. Chem.* 48 (2005) 6012–6022.
 - [27] R.W. Homer, J. Swanson, R.J. Jilek, T. Hurst, R.D. Clark, SYBYL line notation (SLN): a single notation to represent chemical structures, queries, reactions, and virtual libraries, *J. Chem. Inf. Model.* 48 (2008) 2294–2307.
 - [28] A.N. Jain, Surflex: fully automatic flexible molecular docking using a molecular similarity-based search engine, *J. Med. Chem.* 46 (2003) 499–511.
 - [29] R.B. Huang, Q.S. Du, C.H. Wang, K.C. Chou, An in-depth analysis of the biological functional studies based on the NMR M2 channel structure of influenza A virus, *Biochem. Biophys. Res. Commun.* 377 (2008) 1243–1247.
 - [30] K.C. Chou, D.Q. Wei, W.Z. Zhong, Binding mechanism of coronavirus main proteinase with ligands and its implication to drug design against SARS, *Biochem. Biophys. Res. Commun.* 308 (2003) 148–151.
 - [31] Q. Du, S. Wang, D. Wei, S. Sirois, K.C. Chou, Molecular modeling and chemical modification for finding peptide inhibitor against severe acute respiratory syndrome coronavirus main proteinase, *Anal. Biochem.* 337 (2005) 262–270.
 - [32] Q.S. Du, R.B. Huang, C.H. Wang, X.M. Li, K.C. Chou, Energetic analysis of the two controversial drug binding sites of the M2 proton channel in influenza A virus, *J. Theor. Biol.* 259 (2009) 159–164.
 - [33] H. Wei, C.H. Wang, Q.S. Du, J. Meng, K.C. Chou, Investigation into adamantane-based M2 inhibitors with FB-QSAR, *Med. Chem.* 5 (2009) 305–317.
 - [34] Q.S. Du, R.B. Huang, S.Q. Wang, K.C. Chou, Designing inhibitors of M2 proton channel against H1N1 swine influenza virus, *PLoS One* 5 (2010) e9388.
 - [35] S.Q. Wang, Q.S. Du, R.B. Huang, D.W. Zhang, K.C. Chou, Insights from investigating the interaction of oseltamivir (Tamiflu) with neuraminidase of the 2009 H1N1 swine flu virus, *Biochem. Biophys. Res. Commun.* 386 (2009) 432–436.
 - [36] L. Cai, Y. Wang, J.F. Wang, K.C. Chou, Identification of proteins interacting with human SP110 during the process of viral infections, *Med. Chem.* 7 (2011) 121–126.
 - [37] Q.H. Liao, Q.Z. Gao, J. Wei, K.C. Chou, Docking and molecular dynamics study on the inhibitory activity of novel inhibitors on epidermal growth factor receptor (EGFR), *Med. Chem.* 7 (2011) 24–31.
 - [38] C. Bissantz, G. Folkers, D. Rognan, Protein-based virtual screening of chemical databases. 1. Evaluation of different docking/scoring combinations, *J. Med. Chem.* 43 (2000) 4759–4767.
 - [39] G.M. Sastry, M. Adzhigirey, T. Day, R. Annabhimoju, W. Sherman, Protein and ligand preparation: parameters, protocols, and influence on virtual screening enrichments, *J. Comput.-Aided Mol. Des.* 27 (2013) 221–234.
 - [40] S.S. Rozenel, J.B. Kerr, J. Arnold, Metal complexes of Co, Ni and Cu with the pincer ligand HN(CH₂CH₂P(i)Pr₂)₂: preparation, characterization and electrochemistry, *Dalton Trans.* 40 (2011) 10397–10405.
 - [41] J. Xu, Y.F. Ma, W.S. Liu, Y. Tang, M.Y. Tan, Preparation, crystal structures and luminescent properties of terbium and europium complexes with a new amino-alkenone type ligand, *J. Fluorescence* 21 (2011) 35–42.
 - [42] R.D. Clark, A. Strizhev, J.M. Leonard, J.F. Blake, J.B. Matthews, Consensus scoring for ligand/protein interactions, *J. Mol. Graphics Modell.* 20 (2002) 281–295.
 - [43] X. Wu, S. Wu, W.H. Chen, Molecular docking and 3D-QSAR study on 4-(1H-indazol-4-yl) phenylamino and aminopyrazolopyridine urea derivatives as kinase insert domain receptor (KDR) inhibitors, *J. Mol. Model.* 18 (2012) 1207–1218.
 - [44] J. Ruppert, W. Welch, A.N. Jain, Automatic identification and representation of protein binding sites for molecular docking, *Protein Sci.* 6 (1997) 524–533.
 - [45] J. Zhang, C.H. Luan, K.C. Chou, G.V. Johnson, Identification of the N-terminal functional domains of Cdk5 by molecular truncation and computer modeling, *Proteins* 48 (2002) 447–453.
 - [46] J.F. Wang, D.Q. Wei, L. Li, S.Y. Zheng, Y.X. Li, K.C. Chou, 3D structure modeling of cytochrome P450 2C19 and its implication for personalized drug design, *Biochem. Biophys. Res. Commun.* 355 (2007) 513–519.
 - [47] R.M. Pielak, J.R. Schnell, J.J. Chou, Mechanism of drug inhibition and drug resistance of influenza A M2 channel, *Proc. Natl. Acad. Sci. U.S.A.* 106 (2009) 7379–7384.
 - [48] W. Welch, J. Ruppert, A.N. Jain, Hammerhead: fast, fully automated docking of flexible ligands to protein binding sites, *Chem. Biol. Interact.* 3 (1996) 449–462.
 - [49] K.C. Chou, Low-frequency collective motion in biomacromolecules and its biological functions, *Biophys. Chem.* 30 (1988) 3–48.
 - [50] M.R. Housaindokht, M.R. Bozorgmehr, M. Bahrololoom, Analysis of ligand binding to proteins using molecular dynamics simulations, *J. Theor. Biol.* 254 (2008) 294–300.
 - [51] K.C. Chou, Low-frequency resonance and cooperativity of hemoglobin, *Trends Biochem. Sci.* 14 (1989) 212–213.
 - [52] S.-X. Lin, J. Lapointe, Theoretical and experimental biology in one —A symposium in honour of Professor Kuo-Chen Chou's 50th anniversary and Professor Richard Gieg's 40th anniversary of their scientific careers, *J. Biomed. Sci. Eng.* 06 (2013) 435–442.
 - [53] C. Oostenbrink, T.A. Soares, N.F. van der Vegt, W.F. van Gunsteren, Validation of the 53A6 GROMOS force field, *Eur. Biophys. J.* 34 (2005) 273–284.
 - [54] A.W. Schuttelkopf, D.M. van Aalten, PRODRG: a tool for high-throughput crystallography of protein-ligand complexes, *Acta Crystallogr. D: Biol. Crystallogr.* 60 (2004) 1355–1363.
 - [55] Y. Wu, H.L. Tepper, G.A. Voth, Flexible simple point-charge water model with improved liquid-state properties, *J. Chem. Phys.* 124 (2006) 024503.
 - [56] F.W. Starr, J.K. Nielsen, H.E. Stanley, Hydrogen-bond dynamics for the extended simple point-charge model of water, *Phys. Rev. E: Stat. Nonlinear Soft Matter Phys.* 62 (2000) 579–587.
 - [57] J.A. Plumb, P.W. Finn, R.J. Williams, M.J. Bandara, M.R. Romero, C.J. Watkins, N.B. La Thangue, R. Brown, Pharmacodynamic response and inhibition of growth of human tumor xenografts by the novel histone deacetylase inhibitor PXD101, *Mol. Cancer Ther.* 2 (2003) 721–728.
 - [58] W. Shao, J.D. Grownay, Y. Feng, G. O'Connor, M. Pu, W. Zhu, Y.M. Yao, P. Kwon, S. Fawell, P. Atadja, Activity of deacetylase inhibitor panobinostat (LBH589) in cutaneous T-cell lymphoma models: defining molecular mechanisms of resistance, *Int. J. Cancer* 127 (2010) 2199–2208.
 - [59] J. Leyton, J.P. Alao, M. Da Costa, A.V. Stavropoulou, J.R. Latigo, M. Perumal, R. Pillai, Q. He, P. Atadja, E.W. Lam, P. Workman, D.M. Vigushin, E.O. Aboagye, In vivo biological activity of the histone deacetylase inhibitor LAQ824 is detectable with 3'-deoxy-3'-[18F]fluorothymidine positron emission tomography, *Cancer Research* 66 (2006) 7621–7629.
 - [60] J. Cheng, X.L. Ju, X.Y. Chen, G.Y. Liu, Homology modeling of human alpha 1 beta 2 gamma 2 and house fly beta 3 GABA receptor channels and Surflex-docking of fipronil, *J. Mol. Model.* 15 (2009) 1145–1153.
 - [61] J. Sun, S. Cai, H. Mei, J. Li, N. Yan, Y. Wang, Docking and 3D QSAR study of thiourea analogs as potent inhibitors of influenza virus neuraminidase, *J. Mol. Model.* 16 (2010) 1809–1818.
 - [62] P. Mukherjee, A. Pradhan, F. Shah, B.L. Tekwani, M.A. Avery, Structural insights into the Plasmodium falciparum histone deacetylase 1 (PfHDAC-1): a novel target for the development of antimalarial therapy, *Bioorg. Med. Chem.* 16 (2008) 5254–5265.
 - [63] C.A. Lipinski, F. Lombardo, B.W. Dominy, P.J. Feeney, Experimental and computational approaches to estimate solubility and permeability in drug discovery and development settings, *Advanced Drug Delivery Reviews* 46 (2001) 3–26.
 - [64] D.F. Wang, P. Helquist, N.L. Wiech, O. Wiest, Toward selective histone deacetylase inhibitor design: homology modeling, docking studies, and molecular

- dynamics simulations of human class I histone deacetylases, *J. Med. Chem.* 48 (2005) 6936–6947.
- [65] P. de Hoog, L.D. Pachon, P. Gamez, M. Lutz, A.L. Spek, J. Reedijk, Solution-stable trinuclear zinc(II) cluster from 4-methyl-2-N-(2-pyridylmethylene)aminophenol (HPyrimol), *Dalton Trans.* (2004) 2614–2615.
- [66] R. Taylor, Life-science applications of the Cambridge Structural Database, *Acta Crystallogr. D: Biol. Crystallogr.* 58 (2002) 879–888.
- [67] G. Feng, L. Evangelisti, L.B. Favero, J.U. Grabow, Z. Xia, W. Caminati, On the weak O—H...halogen hydrogen bond: a rotational study of CH₃CHClF...H₂O, *Phys. Chem. Chem. Phys.* 13 (2011) 14092–14096.
- [68] A.M. Brzozowski, A.C. Pike, Z. Dauter, R.E. Hubbard, T. Bonn, O. Engstrom, L. Ohman, G.L. Greene, J.A. Gustafsson, M. Carlquist, Molecular basis of agonism and antagonism in the oestrogen receptor, *Nature* 389 (1997) 753–758.
- [69] S.P. Williams, P.B. Sigler, Atomic structure of progesterone complexed with its receptor, *Nature* 393 (1998) 392–396.
- [70] B. Eghdamian, K. Ghose, Mode of action and adverse effects of lipid lowering drugs, *Drugs Today* 34 (1998) 943–956.
- [71] W.J. Egan, G. Lauri, Prediction of intestinal permeability, *Adv. Drug Delivery Rev.* 54 (2002) 273–289.